Acta Crystallographica Section F
Structural Biology and Crystallization Communications
ISSN 1744-3091

Structure of the heterotrimeric PCNA from *Sulfolobus solfataricus*

Gareth J. Williams, Kenneth Johnson, Jana Rudolf, Stephen A. McMahon, Lester Carter, Muse Oke, Huanting Liu, Garry L. Taylor, Malcolm F. White and James H. Naismith*

Centre for Biomolecular Science and The Scottish Structural Proteomics Facility, The University of St Andrews, Fife KY16 9RH, Scotland

Correspondence e-mail: naismith@st-and.ac.uk

Received 6 July 2006
Accepted 24 August 2006

PDB Reference: PCNA, 2ix2, r2ix2sf.

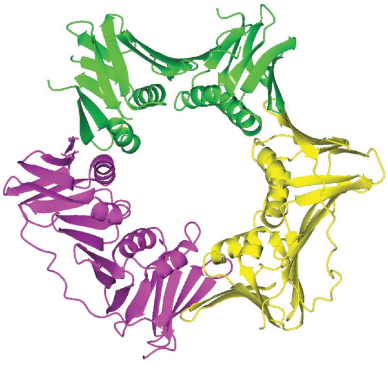

PCNA is a ring-shaped protein that encircles DNA, providing a platform for the association of a wide variety of DNA-processing enzymes that utilize the PCNA sliding clamp to maintain proximity to their DNA substrates. PCNA is a homotrimer in eukaryotes, but a heterotrimer in crenarchaea such as *Sulfolobus solfataricus*. The three proteins are *Sso*PCNA1 (249 residues), *Sso*PCNA2 (245 residues) and *Sso*PCNA3 (259 residues). The heterotrimeric protein crystallizes in space group $P2_1$, with unit-cell parameters a = 44.8, b = 78.8, c = 125.6 Å, $\beta = 100.5^\circ$. The crystal structure of this heterotrimeric PCNA molecule has been solved using molecular replacement. The resulting structure to 2.3 Å sheds light on the differential stabilities of the interactions observed between the three subunits and the specificity of individual subunits for partner proteins.

1. Introduction

PCNA (proliferating cell nuclear antigen) is a trimeric ring-shaped protein that encircles DNA. PCNA acts as a processivity factor, or sliding clamp, for a wide variety of proteins that act on DNA, including DNA polymerases, DNA ligase, endonucleases and glycosylases (reviewed in Warbrick, 2000). In general, these are proteins that act on DNA structures rather than binding to specific sequences and PCNA is thought to help maintain contact with DNA over thousands of nucleotides (Kelman & Hurwitz, 1998). Partner proteins interact with PCNA *via* a PIP-box peptide that makes contact with the interdomain-connecting loop (IDCL) of PCNA (Fig. 1) and up to three different proteins could potentially be loaded onto a single PCNA trimer simultaneously, suggesting that PCNA can act as a molecular 'tool-belt'.

PCNA is conserved in the archaea, which have information-processing pathways that are often simplified versions of those found in eukaryotes. Whilst most archaea encode a homotrimeric PCNA molecule like the eukaryotic version, the crenarchaeote *Sulfolobus solfataricus* and other *Sulfolobus* species possess a heterotrimeric PCNA (*Sso*PCNA; Dionne *et al.*, 2003). This increased complexity allows the opportunity for each subunit to evolve selectivity for binding partners and this has been shown to be the case (Dionne *et al.*, 2003; Dionne & Bell, 2005; Roberts *et al.*, 2003). The heterotrimeric structure of *Sso*PCNA assembles *via* a strong interaction between PCNA subunits 1 and 2, followed by a much weaker interaction with subunit 3 to complete the circle (Dionne *et al.*, 2003), and clamp-loading machinery is not required *in vitro* for assembly on DNA substrates with blocked ends (Roberts & White, 2005). Here, we report the crystal structure of the PCNA heterotrimer from *S. solfataricus* to 2.3 Å.

2. Experimental procedures

The three subunits of PCNA from *S. solfataricus* were expressed in *Escherichia coli* from expression plasmids obtained from the laboratory of Dr Stephen Bell (Dionne *et al.*, 2003). *Sso*PCNA1, *Sso*PCNA2 and *Sso*PCNA3 were overexpressed using the same conditions. *E. coli* Rosetta (DE3) cells, a BL21 (DE3) derivative which contains a plasmid (pRARE) containing the six rare-codon tRNAs for the codons AGG, AGA, AUA, CUA, CCC and GGA,

were transformed with plasmid DNA encoding the target protein. The Rosetta (DE3) cell line enhances the expression of genes in *E. coli* that contain codons not commonly found in *E. coli*. Single colonies were grown in 10 ml LB supplemented with 50 µg ml^{-1} kanamycin overnight. Overnight cultures were used to inoculate 500 ml LB supplemented with 50 µg ml^{-1} kanamycin in 2 l flasks. Cells were grown to an OD_{600} of 0.8–1.0 at 310 K and then induced with 0.2 m*M* isopropyl β-D-thiogalactopyranoside at 291 K overnight. Cells were harvested at 10 500*g* and resuspended in equilibration buffer (50 m*M* HEPES pH 8.0, 10 m*M* imidazole and 300 m*M* NaCl). Soluble proteins were extracted by incubation at room temperature for 1 h with 100 µg ml^{-1} lysozyme and 20 µg ml^{-1} DNase (Sigma), followed by two passes through a constant cell disruptor (Constant systems) and subsequent centrifugation for 30 min at 75 500*g*. The purification protocols of *Sso*PCNA1, *Sso*PCNA2 and *Sso*PCNA3 are essentially identical. Supernatant containing target protein was applied onto a charged HisTrap Nickel Sepharose high-performance column (GE Healthcare) pre-equilibrated with equilibration buffer and weakly bound proteins were removed by extensive washing with buffer containing 50 m*M* and then 100 m*M* imidazole. Essentially pure target protein was eluted with 250 m*M* imidazole, dialyzed into 50 m*M* HEPES pH 8.0 containing 250 m*M* NaCl and further purified by Superdex S200 gel-filtration chromatography (GE Healthcare). The three PCNA subunits were then mixed in an approximately equimolar ratio and incubated at room temperature for 1 h; the PCNA heterotrimer was then purified by S200 gel filtration. Each step of purification was monitored by SDS–PAGE. After the gel-filtration step proteins were judged to be pure by Coomassie-stained gels and their integrity was confirmed by mass spectrometry. The pure PCNA heterotrimer was concentrated to 15 mg ml^{-1} and dialyzed into 20 m*M* HEPES pH 7.5, 20 m*M* NaCl and 2 m*M* DTT prior to crystallization.

The protein was screened for crystallization in sitting-drop vapour-diffusion experiments using a Cartesian nano-dispensing robot (Genomic Solutions) against a wide range of sparse-matrix screens. Conditions which gave crystals were scaled up and optimized by systematic variation of the conditions. The best crystals were obtained from sitting-drop vapour diffusion of 1 µl protein solution with 1 µl 7.5% PEG 20 000 against a 100 µl reservoir of 7.5% PEG 20 000. The crystals form thin sheets that cluster together. However, careful manipulation allowed the removal of a single crystal, which was cryoprotected with 20% (2*R*,3*R*)-(−)2,3-butanediol (Sigma) prior to X-ray diffraction at 100 K. Data to 2.3 Å were collected on a single PCNA heterotrimer crystal at Daresbury synchrotron-radiation source, beamline 14.1. 350 diffraction images with 0.4° oscillation range were collected using a Quantum 4 ADSC detector, an exposure time of 25 s and a crystal-to-detector distance of 95 mm, with a wavelength of 1.488 Å. Data were indexed and scaled with *HKL*-2000 (Otwinowski & Minor, 1997). Full details are given in Table 1; no cutoff was applied and the Wilson *B* factor is estimated as 46 Å^2. The structure was solved by molecular replacement using *Phaser* (McCoy *et al.*, 2005; Storoni *et al.*, 2004) as implemented in *CCP*4 (Collaborative Computational Project, Number 4, 1994) using the monomer from *S. tokadaii* (PDB code 1ud9) as the search model. Each subunit was found separately, with *Z* scores of 9.1 (*Sso*PCNA1), 10.4 (*Sso*PCNA2) and 8.1 (*Sso*PCNA3). The structure was refined

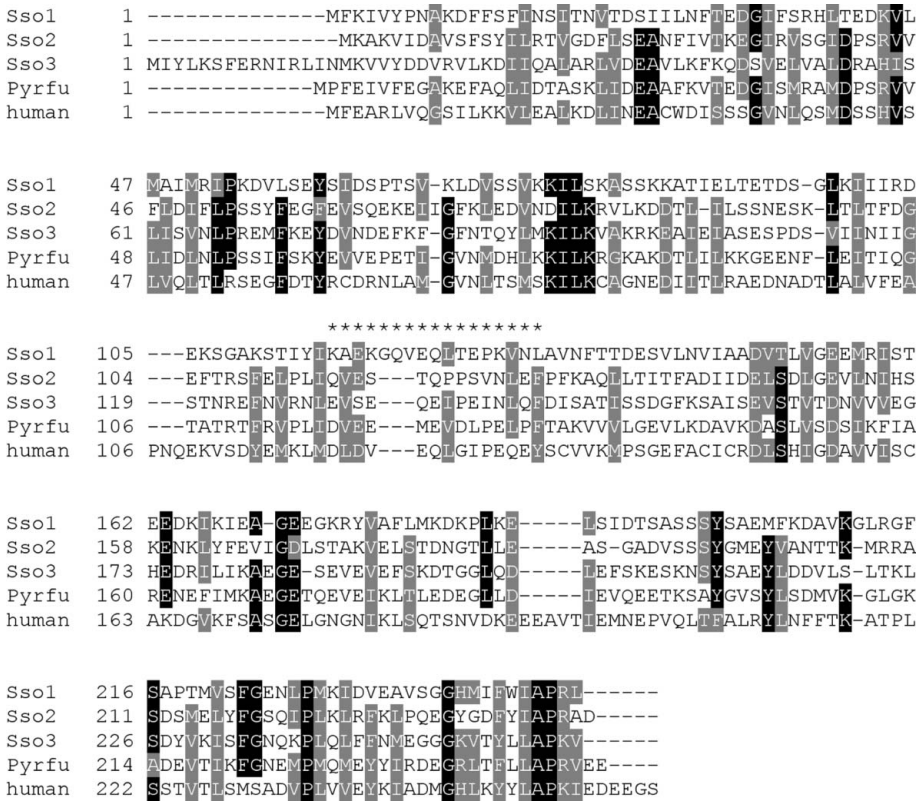

Figure 1
Sequence alignment of the three *Sso*PCNA subunits with the single PCNA proteins from *Pyrococcus furiosus* and *Homo sapiens*. Highly conserved residues are highlighted in black and conservatively substituted residues in grey. The interdomain-connecting loop (IDCL) is indicated by asterisks, highlighting the three-residue insertion present in *Sso*PCNA1. The sequence given for *Sso*PCNA3 is that used in this study and is based on its original annotation in the public database. The second M (residue 16) is probably the correct start site. Accession Nos.: *Sso*PCNA1, P57766; *Sso*PCNA2, Q97Z84; *Sso*PCNA3, P57765; *Sto*PCNA3, Q975N2; *P. furiosus Pyrfu*PCNA, O73947; human PCNA, P12004.

Table 1
Crystallographic data for *Sso*PCNA.

Values in parentheses refer to the highest resolution shell.

Beamline	Daresbury 14.1
Wavelength (Å)	1.48
Resolution (Å)	60.00–2.20 (2.28–2.20)
Space group	$P2_1$
Temperature (K)	100
Detector	Quantum 4 ADSC
Unit-cell parameters (Å, °)	a = 44.8, b = 78.8, c = 125.6, $\alpha = \gamma = 90$, $\beta = 100.5$
Solvent content (%)	52.48
Unique reflections	43983 (4117)
$I/\sigma(I)$	13.4 (1.9)
Average redundancy	2.3 (2.2)
Data completeness (%)	91.2 (93.9)
R_{merge}† (%)	0.060 (0.384)
Refinement	
R factor (%)	21.7 (24.3)
R_{free} (%)	27.3 (28.7)
R.m.s.d. bond distance (Å)	0.015
R.m.s.d. bond angle (°)	1.35
Average B factors (Å^2)	
Main chain	54.63
Side chain	55.89
Solvent	54.44
Ramachandran plot (%)	
Core	98
Disallowed	0
No. of protein atoms	5583
No. of solvent atoms	121
PDB code	2ix2

† $R_{merge} = \sum\sum I(h)_i - \langle I(h)\rangle|/\sum I(h)_i$, where $I(h)$ is the measured diffraction intensity and the summation includes all observations. † R factor = $\sum||F_o| - |F_c||/\sum|F_o|$. ‡ R_{free} is calculated the same way as R factor for data omitted from refinement (5% of reflections for all data sets).

using *REFMAC*5 (Murshudov *et al.*, 1997, 1999) and manually rebuilt with *Coot* (Emsley & Cowtan, 2004). The simulated-annealing protocol in *CNS* (Brünger *et al.*, 1998) and *XFIT* (McRee, 1999) were used to help with fitting difficult loops. The structure was examined with *MOLPROBITY* (Davis *et al.*, 2004). The number of residues observed for chains *A*, *B* and *C* were 226, 245 and 241, respectively. Chain *A* is missing the N-terminal methionine, three short loops comprising residues 84–85, 93–95 and 172–175 and the long IDCL comprising residues 117–130. Chain *B* is complete, whereas chain *C* is missing the first nine N-terminal residues and two short loops comprising residues 183–186 and 197–201. In addition, the structure contains 121 modelled water molecules. Figures were produced with the *CCP*4 viewer (Potterton *et al.*, 2004).

Table 2
The sequence identity/similarity (%) between PCNA molecules.

	*Sso*PCNA1	*Sso*PCNA2	*Sso*PCNA3	*hu*PCNA	*Sto*PCNA3	*Pyrfu*PCNA
*Sso*PCNA1		24/39	17/39	16/42	20/40	21/43
*Sso*PCNA2			23/48	21/45	26/51	31/54
*Sso*PCNA3				24/46	61/82	31/56
*hu*PCNA					23/47	24/48
*Sto*PCNA3						29/52

3. Results

The structure consists of three monomers, *Sso*PCNA1, *Sso*PCNA2 and *Sso*PCNA3 (denoted monomers *A*, *B* and *C*, respectively, in the crystal structure), which share only ∼22% sequence identity (Table 2). The three monomers share a similar fold, although there are important differences in detail which are discussed later. Each monomer of *Sso*PCNA has two domains which are themselves structural duplicates. The fold of the monomer (and domains) is unchanged from the description of the yeast protomer (Krishna *et al.*, 1994). Briefly, each monomer has two lobes. Each lobe is shaped like a triangle, with two sides being formed by β-sheets and one by two α-helices. One of the β-sheets pairs with the β-sheet of the other domain, making an extended β-sheet (Fig. 2). The *Sso*PCNA heterotrimer has the same apparent threefold symmetry observed in the homotrimeric structure first found in the structure from yeast

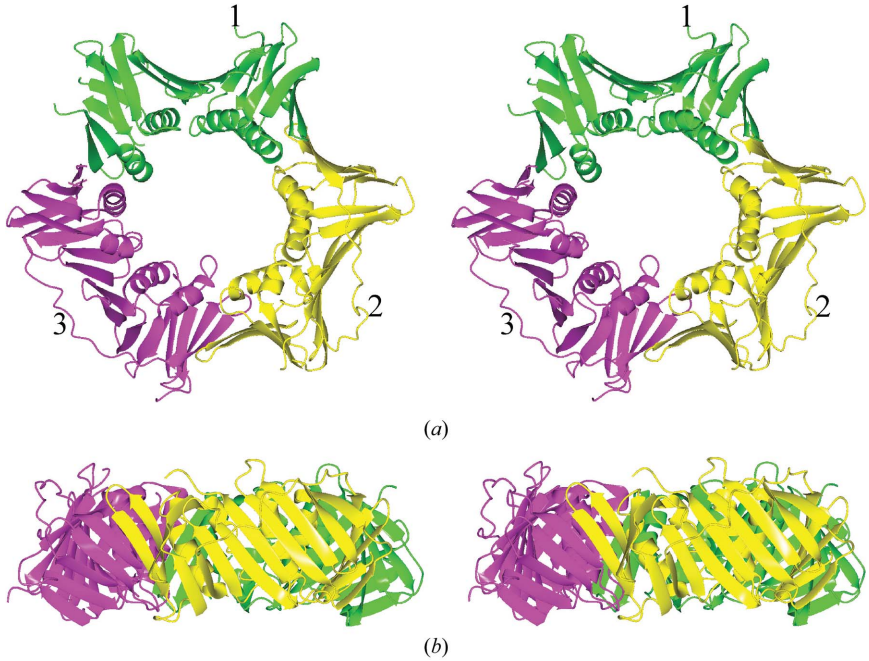

Figure 2
(*a*) A stereoview ribbon representation of the *Sso*PCNA hetereotrimer. *Sso*PCNA1 is coloured green, *Sso*PCNA2 yellow and *Sso*PCNA3 magenta. This view looks down on the 'top' of the structure. The IDCL is marked with a 1 for *SSo*PCNA1, 2 for *SSo*PCNA2 and 3 for *Sso*PCNA3. (*b*) The molecule has been rotated 90° relative to the orientation in (*a*).

Table 3
Structural similarity between PCNA molecules.

The r.m.s.d. (Å) and number of C^{α} atoms are listed. The values were calculated using secondary-structure matching as implemented in *CCP*4 (Collaborative Computational Project, Number 4, 1994).

	*Sso*PCNA1	*Sso*PCNA2	*Sso*PCNA3	*hu*PCNA	*Sto*PCNA3
*Sso*PCNA1		2.0/210	2.2/203	1.9/214	2.1/208
*Sso*PCNA2			1.4/228	1.8/210	1.5/220
*Sso*PCNA3				1.7/226	1.3/224

(Krishna *et al.*, 1994). In the heterotrimer, the threefold symmetry is not perfect. The apparent 'threefold' rotational symmetry of the trimer means that each PCNA molecule interacts with the other two monomers (Fig. 2). The N-terminal lobe of *Sso*PCNA1 interacts with the C-terminal lobe of *Sso*PCNA3, the C-terminal lobe of *Sso*PCNA1 with the N-terminal lobe of *Sso*PCNA2 and the C-terminal lobe of *Sso*PCNA2 with the N-terminal lobe of *Sso*PCNA3. There are no solvent molecules which mediate the contacts between the subunits. We define the top of the ring as the face where the C-termini are located (Fig. 2).

In each of the three monomers, about 100 C^{α} atoms of the N-terminal domain can be superimposed with a root-mean-square deviation (r.m.s.d.) of 2.0 Å on the C-terminal domain. This gives the heterotrimer a pseudo-sixfold symmetric appearance. The complete monomers of *Sso*PCNA2 and *Sso*PCNA3 are well ordered, but the N-terminal 120 residues (essentially the N-terminal lobe) of *Sso*PCNA1 are only weakly ordered, suggesting this domain is mobile in the complex. Comparing the monomers reveals (Table 3) that *Sso*PCNA1 stands out as distinct from the other monomers (even if superposition is restricted to domains). Comparison of the monomers with a recent structure of the homotrimeric human PCNA molecule (*hu*PCNA; PDB code 1vym; Kontopidis *et al.*, 2005) reveals that the three monomers are almost equally distinct from *hu*PCNA (r.m.s.d.s of 1.9, 1.8 and 1.7 Å for *Sso*PCNA1, *Sso*PCNA2 and *Sso*PCNA3, respectively). The same conclusion is reached if one superimposes domains rather than monomers. The *S. tokadaii* PCNA3 (*Sto*PCNA3) monomer (PDB code 1ud9; Matsumiya *et al.*, 2001) is of course most similar to *Sso*PCNA3, but once again it is *Sso*PCNA1 which is structurally distinct. *Sto*PCNA3 is found as a homodimer in its crystal structure, which has no relation to the biological heterotrimeric structure observed *in vivo* (Dionne *et al.*, 2003).

The entire *Sso*PCNA heterotrimer can be superimposed onto *hu*PCNA with an r.m.s.d. of 2.2 Å for 640 C^{α} atoms. However, if only *Sso*PCNA1 (or *Sso*PCNA2) is used in calculating the superposition, it can be seen that the *Sso*PCNA3 is shifted with respect to the ring structure (Fig. 3). The shift is both a translation and rotation; the effect is that *Sso*PCNA3 sits around 4 Å above the ring in the heterotrimer compared with the *hu*PCNA homotrimer (Fig. 3). This displacement of *Sso*PCNA3 is manifested in the interfaces in the heterotrimer. The CCP4 Protein Interfaces, Surfaces and Assemblies (PISA) server at the European Bioinformatic Institute (EBI; http://www.ebi.ac.uk/msd-srv/prot_int/pistart.html) is a powerful tool for assessing the thermodynamics of interface formation based on structural data (Krissinel & Henrick, 2005). The program also computes a significance score which has been derived from an analysis of the known complexes in the Protein Data Bank. This tool shows the *Sso*PCNA1–*Sso*PCNA2 interface is largely hydrophobic (and thus favourable) and has a number of specific hydrogen bonds. The interface has a significance of 1 (the highest), indicating the complex is stable and essential for the formation of the trimer. This is in agreement with biological data, which indicated that the *Sso*PCNA1 and *Sso*PCNA2 subunits form a stable dimer in solution (Dionne *et al.*, 2003). The *Sso*PCNA2–*Sso*PCNA3 interface, despite burying a similar amount of surface area to the *Sso*PCNA1–

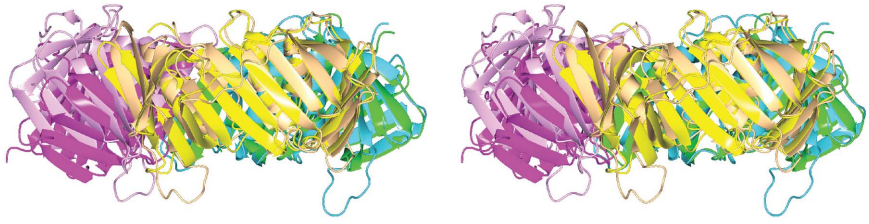

Figure 3
*Sso*PCNA3 is displaced from the ring relative to the observation for the *hu*PCNA homotrimer (PDB code 1vym; Kontopidis *et al.*, 2005). The *Sso*PCNA trimer is coloured as in Fig. 2(*a*); the human trimer is coloured cyan, wheat and pale pink. The same displacement is seen when compared with the yeast homotrimer (Krishna *et al.*, 1994). The structures are shown in stereoview.

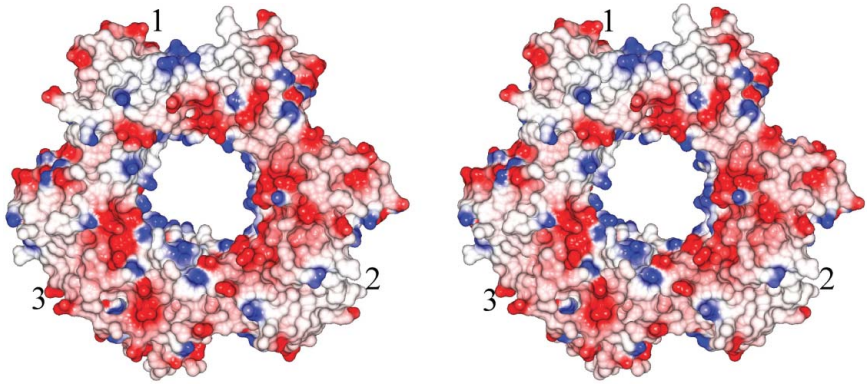

Figure 4
Stereoview of surface properties coloured by electrostatic potential of *Sso*PCNA. The orientation of the molecule is the same as in Fig. 2(*a*). 1 denotes the likely binding site for accessory proteins which bind to *Sso*PCNA1, 2 for *Sso*PCNA2 and 3 for *Sso*PCNA3.

*Sso*PCNA2 interface, has a significance of only 0.24, indicating the complex is context-sensitive, in agreement with biological data (Dionne *et al.*, 2003). This interface, although it has a number of specific hydrogen bonds, is significantly polar and hence less favourable. The *Sso*PCNA1–*Sso*PCNA3 interface has a significance of 0.27, suggesting that it too is context-sensitive and will only form in the presence of the *Sso*PCNA1–*Sso*PCNA2 heterodimer; once again, this agrees with solution data (Dionne *et al.*, 2003), which indicates that *Sso*PCNA3 does not bind strongly to either *Sso*PCNA1 or *Sso*PCNA2 on their own and binds the heterodimer comparatively weakly (Dionne *et al.*, 2003). For comparison, the interfaces in *hu*PCNA have a significance of 0.47, which is in the 'grey' area between stable and unstable. Strikingly, then, the *Sso*PCNA1–*Sso*PCNA2 heterodimer appears to be significantly more stable than even the human homotrimer. The homodimeric interfaces in *Sto*PCNA3 have a significance of 0 (the lowest), agreeing with solution data that these are crystal contacts with no biological relevance (Dionne *et al.*, 2003).

4. Discussion

Peptide soaks and co-complexes of *hu*PCNA (Bruning & Shamoo, 2004; Sakurai *et al.*, 2005; Bowman *et al.*, 2004; Kontopidis *et al.*, 2005) indicate that the accessory proteins bind to the loop which connects the domains within the monomer on top of the trimer, the IDCL. The interaction is centred on Leu126, a conserved hydrophobic residue (Fig. 1). The homotrimer of course presents three identical IDCLs, but the heterotrimer presents three distinct interfaces. These interfaces are known to interact with different proteins, conferring a degree of control of selectivity in crenarchaea that is not possible for the eukaryotic protein (Dionne *et al.*, 2003). In *Sso*PCNA1, the IDCL has an insertion of three amino acids compared with other archaeal and eukaryotic sequences (Fig. 1) and is assumed to be distinct. In our structure, this loop is disordered and cannot be modelled reliably. In *Sso*PCNA2 the IDCL is mainly hydrophobic with a positively charged patch, whereas in *Sso*PCNA3 this region is more negatively charged (Fig. 4). The structure confirms that the heterotrimer does indeed present three different attachment sites. The identity of the interacting residues cannot be inferred from either this structure or from sequence alignment. As would be expected for a molecule which interacts with DNA, the inner surface of the ring is positively charged (*Sso*PCNA1 residues Lys10, Lys81, Lys175, Lys183, Lys206, Lys210; *Sso*PCNA2 residues Arg16, Lys80, Arg81, Lys206, Arg208, Arg209; *SSo*PCNA3 residues Arg24, Lys27, Arg35, Lys91, Lys94, Lys97, Arg98, Lys99, Arg122, Lys155, Lys224). The asymmetry of the heterotrimer is clearly visible when looking at the central hole. This hole is narrower in *Sso*PCNA1 (Fig. 4) than in the other two monomers.

*Sso*PCNA1 appears to be structurally distinct from the other two monomers. It may be that this monomer must be capable of a structural deformation to accommodate *Sso*PCNA3 in forming the heterotrimer. In support of this hypothesis, we make the following observations. Firstly, *Sso*PCNA2 and *Sso*PCNA3 are structurally similar to each other and to *Sto*PCNA3, implying that these monomers are not sensitive to the quite different packing arrangements they find themselves in. The interface between *Sso*PCNA3 and *Sso*PCNA1 is weak and suboptimal, according to analysis of both the crystal structure and solution measurements (Dionne *et al.*, 2003), and this is mirrored by the displacement of *Sso*PCNA3 from the plane of the ring (compared with the human and yeast structures). Finally, the N-terminal domain of *Sso*PCNA1 that is in contact with *Sso*PCNA3 is partly disordered, suggesting that the domain is indeed mobile.

5. Conclusions

The crenarchaeal PCNA molecule is unusual in being more complex than its eukaryotic equivalent. The heterotrimeric organization allows heterogeneity between the three subunits for both inter-subunit interactions and specificity for binding partners. *Sso*PCNA1 and *Sso*PCNA2 form a stable heterodimer that then recruits a third monomer, *Sso*PCNA3, to complete the characteristic ring structure. This third molecule is only weakly bound by the dimer, allowing the functional clamp to disassemble and re-assemble quite easily. *Sso*PCNA1 appears to have a distinct structure and plays the key role in *Sso*PCNA assembly.

The SSPF is funded by the Scottish Funding Council (SFC) and by the Biotechnology Biological Science Research Council (BBSRC) (UK). JHN is a BBSRC career development fellow. We thank John Tainer for support during the work and Steve Bell for the kind gift of the expression plasmids for the three *Sso*PCNA subunits. Thanks to Catherine Botting for mass-spectrometry services.

References

Bowman, G. D., O'Donnell, M. & Kuriyan, J. (2004). *Nature (London)*, **429**, 724–730.
Brünger, A. T., Adams, P. D., Clore, G. M., DeLano, W. L., Gros, P., Grosse-Kunstleve, R. W., Jiang, J.-S., Kuszewski, J., Nilges, M., Pannu, N. S., Read, R. J., Rice, L. M., Simonson, T. & Warren, G. L. (1998). *Acta Cryst.* D**54**, 905–921.
Bruning, J. B. & Shamoo, Y. (2004). *Structure*, **12**, 2209–2219.
Collaborative Computational Project, Number 4 (1994). *Acta Cryst.* D**50**, 760–763.
Davis, I. W., Murray, L. W., Richardson, J. S. & Richardson, D. C. (2004). *Nucleic Acids Res.* **32**, W615–W619.
Dionne, I. & Bell, S. D. (2005). *Biochem. J.* **387**, 859–863.
Dionne, I., Nookala, R. K., Jackson, S. P., Doherty, A. J. & Bell, S. D. (2003). *Mol. Cell*, **11**, 275–282.
Emsley, P. & Cowtan, K. (2004). *Acta Cryst.* D**60**, 2126–2132.
Kelman, Z. & Hurwitz, J. (1998). *Trends Biochem. Sci.* **23**, 236–238.
Kontopidis, G., Wu, S. Y., Zheleva, D. I., Taylor, P., McInnes, C., Lane, D. P., Fischer, P. M. & Walkinshaw, M. D. (2005). *Proc. Natl Acad. Sci. USA*, **102**, 1871–1876.
Krishna, T. S. R., Kong, X. P., Gary, S., Burgers, P. M. & Kuriyan, J. (1994). *Cell*, **79**, 1233–1243.
Krissinel, E. & Henrick, K. (2005). *Lect. Notes Comput. Sci.* **3695**, 163–174.
McCoy, A. J., Grosse-Kunstleve, R. W., Storoni, L. C. & Read, R. J. (2005). *Acta Cryst.* D**61**, 458–464.
McRee, D. E. (1999). *J. Struct. Biol.* **125**, 156–165.
Matsumiya, S., Ishino, Y. & Morikawa, K. (2001). *Protein Sci.* **10**, 17–23.
Murshudov, G. N., Vagin, A. A. & Dodson, E. J. (1997). *Acta Cryst.* D**53**, 240–255.
Murshudov, G. N., Vagin, A. A., Lebedev, A., Wilson, K. S. & Dodson, E. J. (1999). *Acta Cryst.* D**55**, 247–255.
Otwinowski, Z. & Minor, W. (1997). *Methods Enzymol.* **276**, 307–326.
Potterton, L., McNicholas, S., Krissinel, E., Gruber, J., Cowtan, K., Emsley, P., Murshudov, G. N., Cohen, S., Perrakis, A. & Noble, M. (2004). *Acta Cryst.* D**60**, 2288–2294.
Roberts, J. A., Bell, S. D. & White, M. F. (2003). *Mol. Microbiol.* **48**, 361–371.
Roberts, J. A. & White, M. F. (2005). *J. Biol. Chem.* **280**, 5924–5928.
Sakurai, S., Kitano, K., Yamaguchi, H., Hamada, K., Okada, K., Fukuda, K., Uchida, M., Ohtsuka, E., Morioka, H. & Hakoshima, T. (2005). *EMBO J.* **24**, 683–693.
Storoni, L. C., McCoy, A. J. & Read, R. J. (2004). *Acta Cryst.* D**60**, 432–438.
Warbrick, E. (2000). *Bioessays*, **22**, 997–1006.